ADVANCED FUNCTIONAL MATERIALS

Supporting Information

for *Adv. Funct. Mater.*, DOI 10.1002/adfm.202407077

3D-Printing of Highly Piezoelectric Barium Titanate Polymer Nanocomposites with Surface-Modified Nanoparticles at Low Loadings

Mirko Maturi, Lorenzo Migliorini, Sara Moon Villa, Tommaso Santaniello, Natalia Fernandez-Delgado, Sergio Ignacio Molina, Paolo Milani, Alberto Sanz de León* and Mauro Comes Franchini**

Supporting Information

3D-printing of highly piezoelectric nanocomposites with surface-modified barium titanate nanoparticles at low loadings via vat photopolymerization

Mirko Maturi, Lorenzo Migliorini, Sara Moon Villa, Tommaso Santaniello, Natalia Fernandez-Delgado, Sergio Ignacio Molina, Paolo Milani, Alberto Sanz de León* and Mauro Comes Franchini**

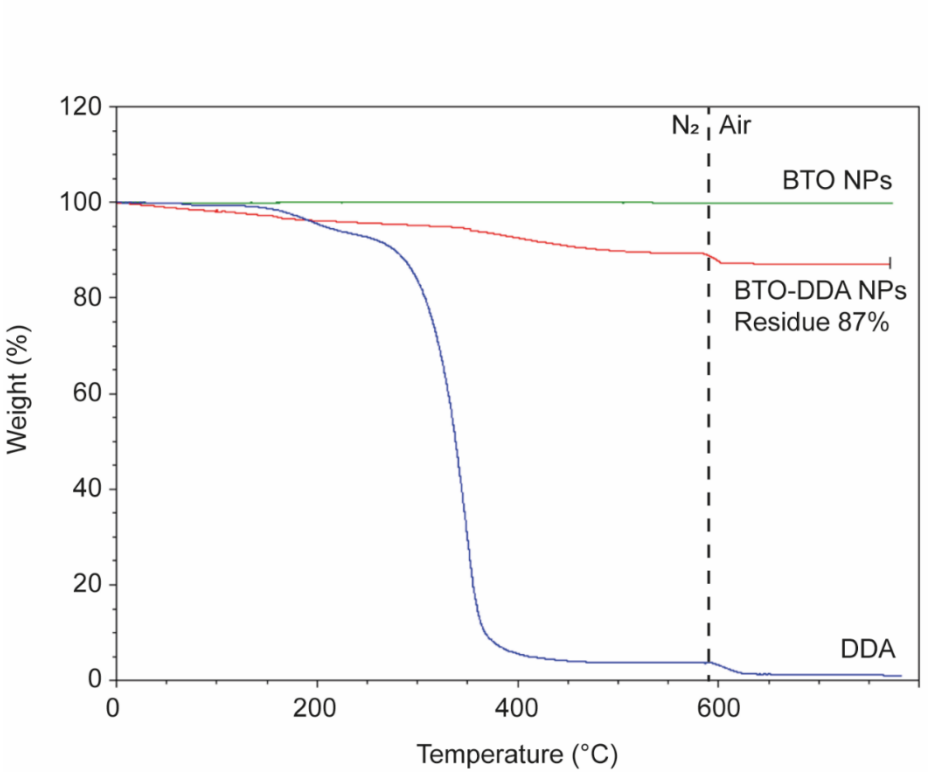

Figure S1. Thermogravimetric analysis (TGA) of unmodified BTO nanoparticles (green curve), DDA ligand (blue curve) and surface-modified BTO-DDA (red curve), revealing a total organic content of 13%. Dashed line corresponds to the switch to air for the gasification of carbonaceous residues, at constant temperature T = 600°C.

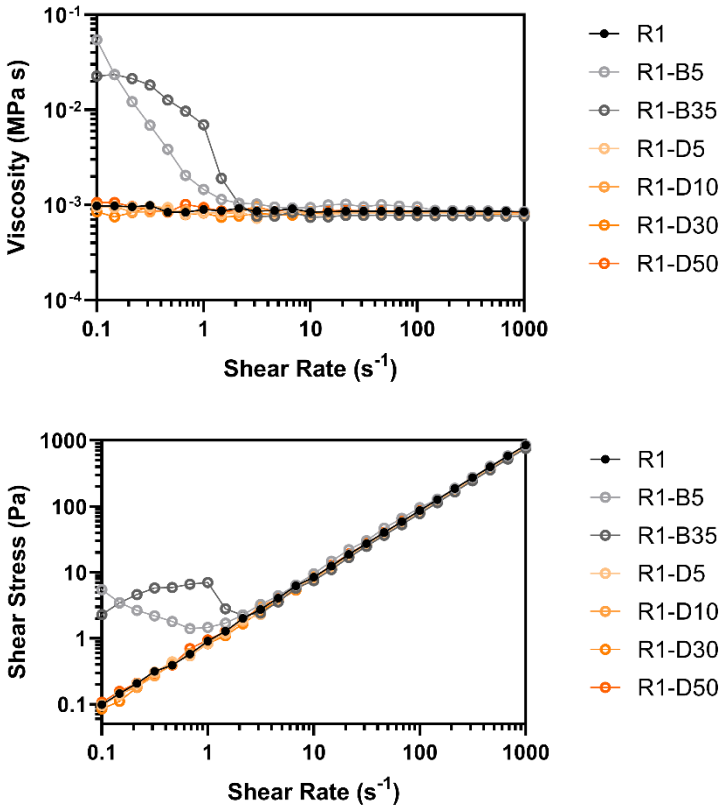

Figure S2. Rheological analysis of formulated 3D printable nanocomposite resins. Influence of shear rate on viscosity (top) and shear stress (bottom).

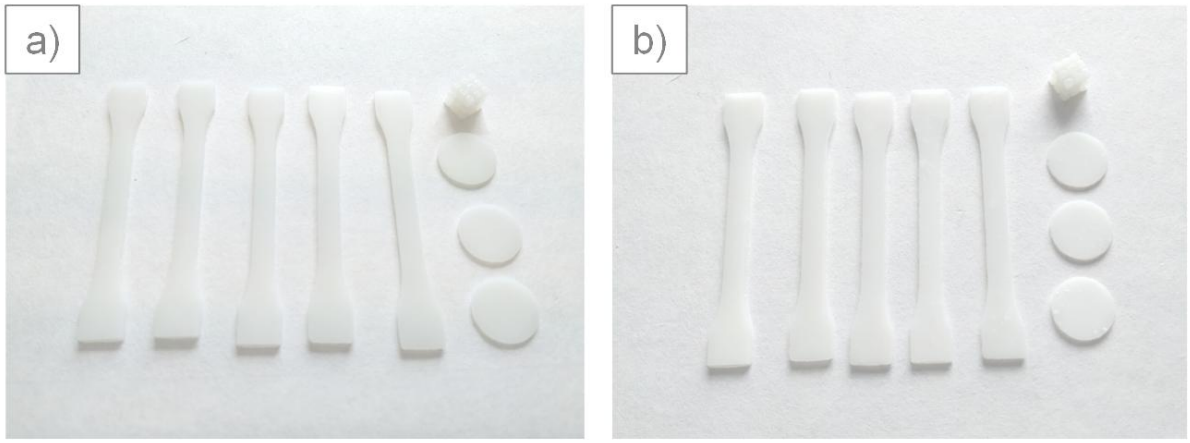

Figure S3. Digital photographs of different objects printed with a) 0.5 wt.% and d) 3.5 wt.% BTO and R1.

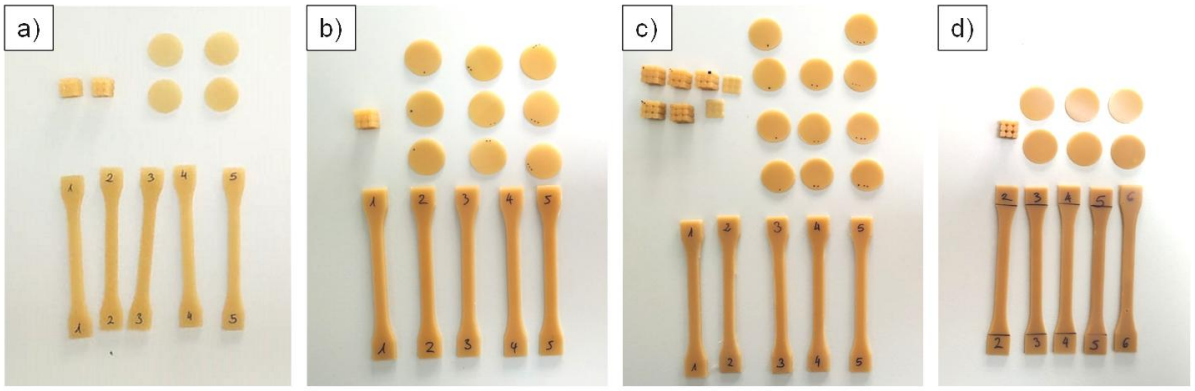

Figure S4. Digital photographs of different objects printed with a) 0.5 wt.%; b) 1.0 wt.%; c) 3.0 wt.% and d) 5.0 wt.% BTO-DDA and R1.

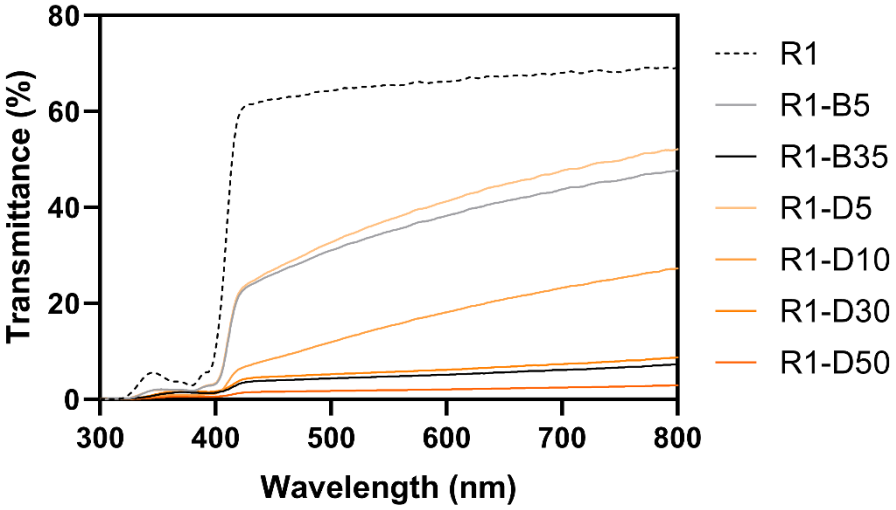

Figure S5. Transmittance measurements of 3D printed discs (thickness = 0.5 mm).

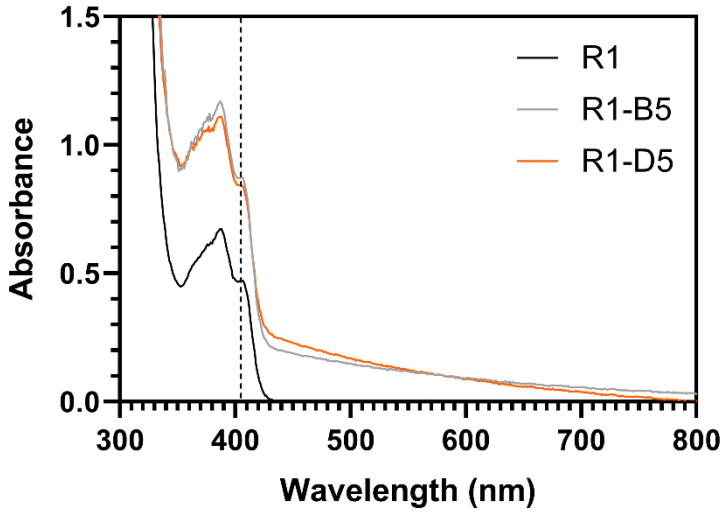

Figure S6. Optical absorption properties of photocurable nanocomposite resins (2 vol.% in DMF). The dashed line corresponds to 405 nm, the emission wavelength of the light source used for 3D printing.

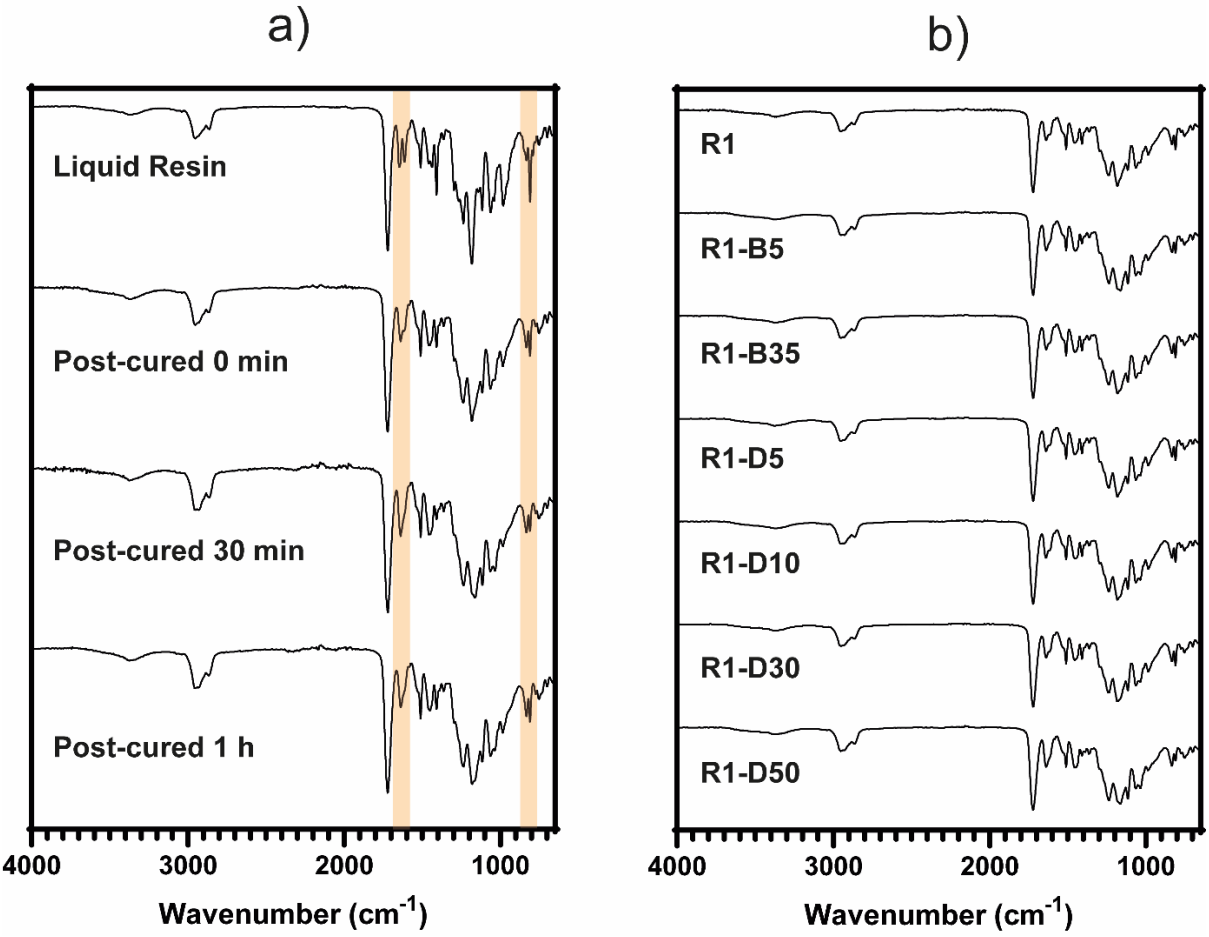

Figure S7. ATR-FTIR spectroscopy. a) R1 resins before printing (Liquid Resin), right after printing (Post-cured 0 min), and after 30 or 60 min of post-curing in a UV chamber at 60°C. b) Formulated resins, recorded right after printing. Colored bands in a) correspond to the regions where it is possible to observe the decrease in the intensity of the vibration bands associated with the photocurable C=C bond.

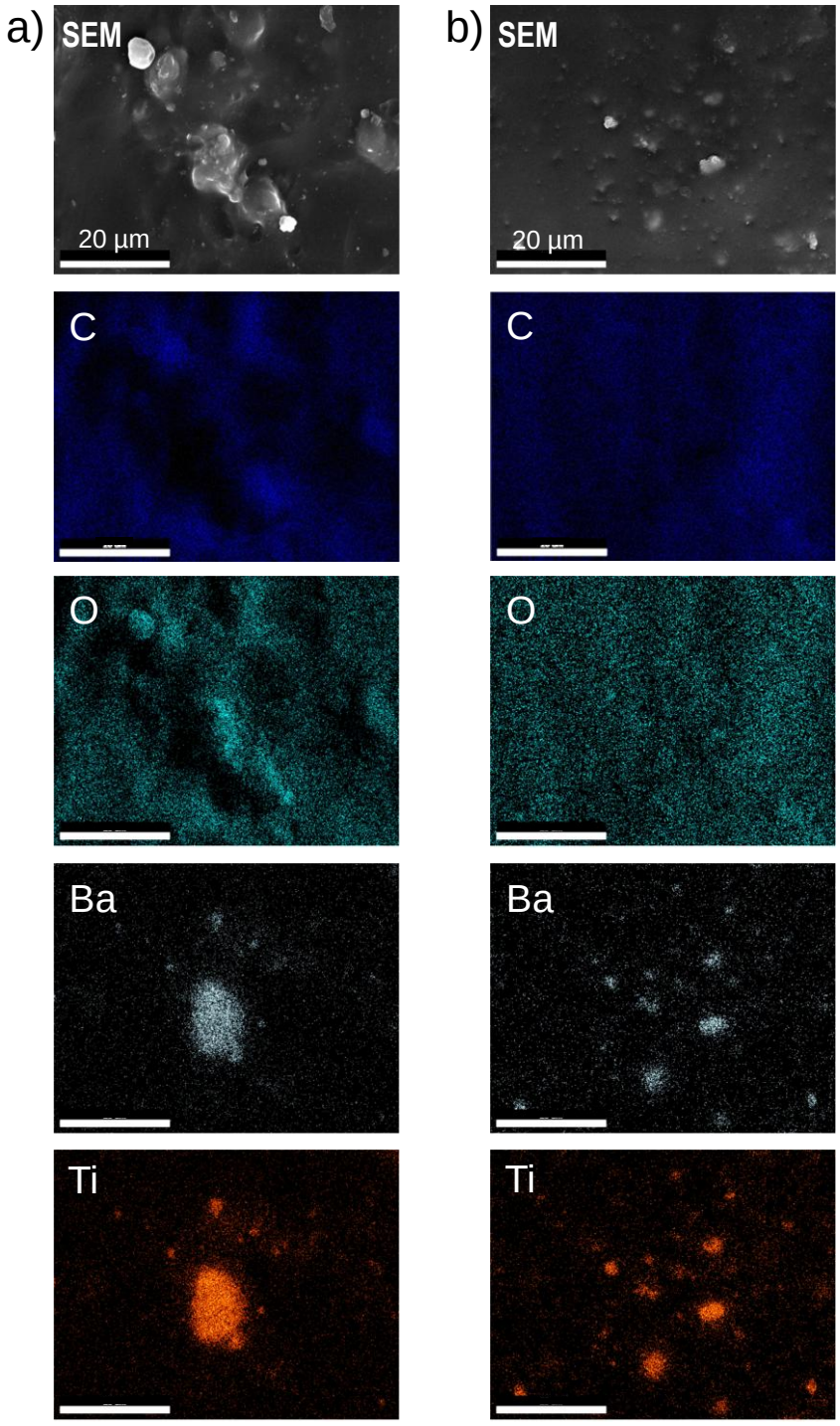

Figure S8. SEM and individual EDX mappings of a) R1-B5 and b) R1-D5 nanocomposites.

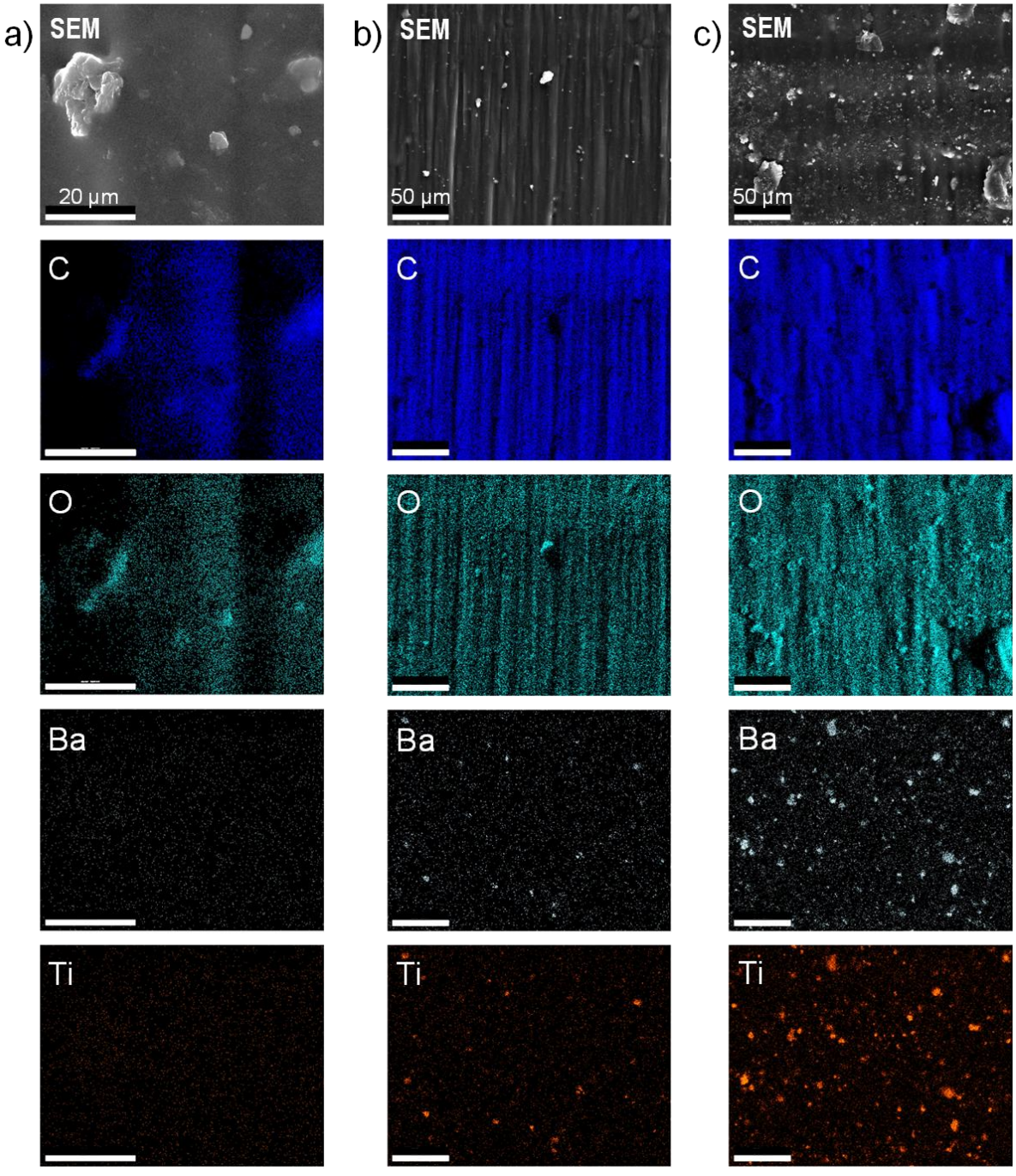

Figure S9. SEM and individual EDX mappings of a) R1; b) R1-D5 and c) R1-D30 nanocomposites.

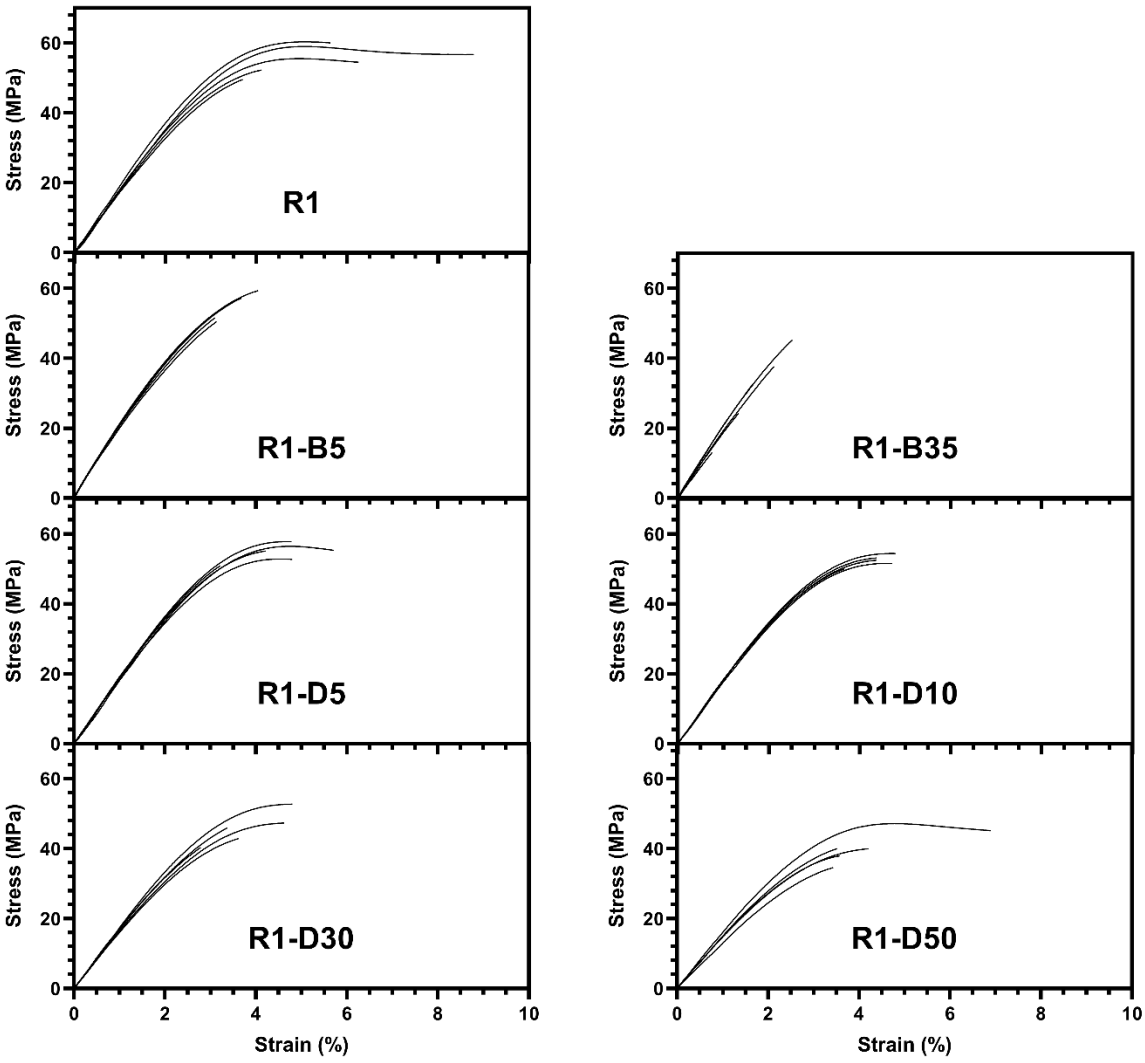

Figure S10. Tensile stress-strain curves for R1 set of resins. $N = 5$ for all samples.

	R2	R2-D5	R2-D10	R2-D23
BTO	-	-	-	-
BTO-DDA	-	0.5 wt.%	1.0 wt.%	2.3 wt.%

Table S1. Composition and designation of the prepared liquid nanocomposites using R2 resin.

	R3	R3-D5	R3-D10	R3-D23	R3-D30
BTO	-	-	-	-	-
BTO-DDA	-	0.5 wt.%	1.0 wt.%	2.3 wt.%	3.0 wt.%

Table S2. Composition and designation of the prepared liquid nanocomposites using R3 resin.

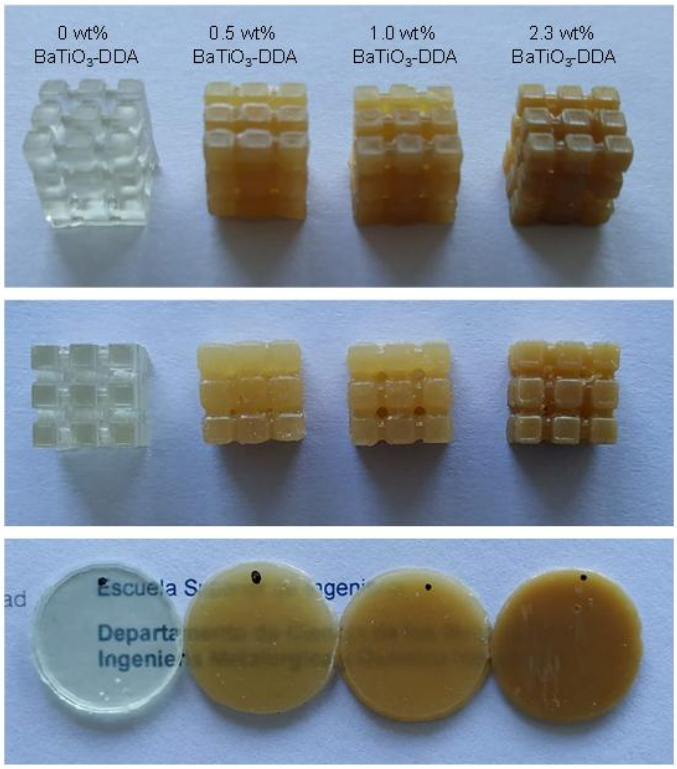

Figure S11. Digital photographs of different objects printed with R2-D5, R2-D10 and R2-D23

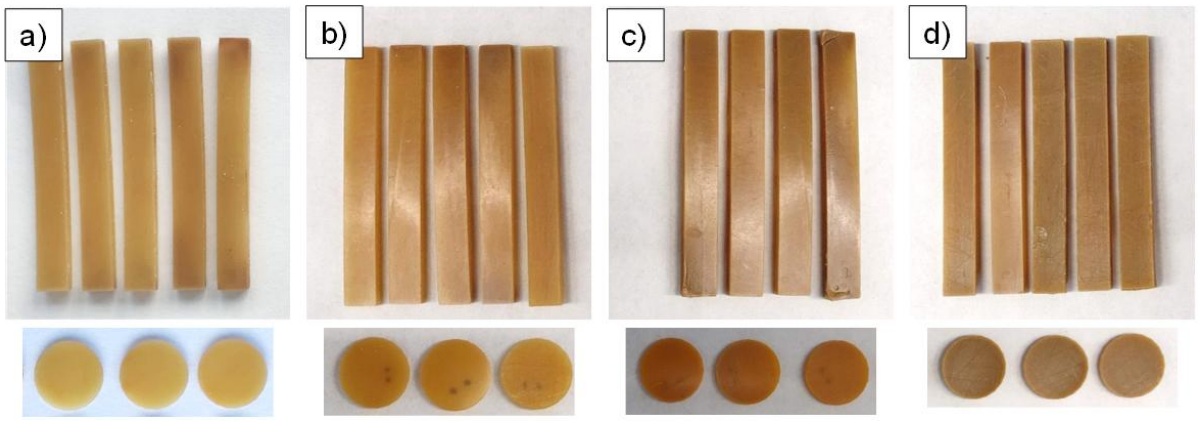

Figure S12. Digital photographs of different objects printed with a) R3-D5, b) R3-D10, c) R3-D23 and d) R3-D30.

Sample	Flexural Modulus (MPa)
R2	3.5 ± 0.2
R2-D5	3.6 ± 0.3
R2-D10	3.8 ± 0.2
R2-D23	3.5 ± 0.5

Table S3 – Flexural modulus of nanocomposites printed with resin R2 as the matrix. Data are expressed as mean ± SD, obtained by averaging five replicate measurements for each composition.

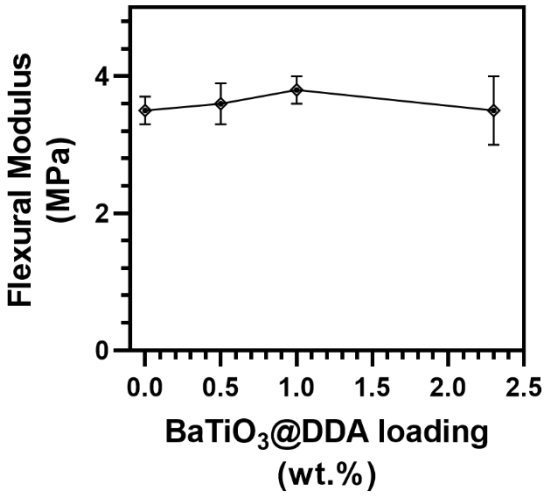

Figure S13. Flexural modulus of BTO-DDA nanocomposites prepared using R2 as polymer matrix as a function of BTO-DDA loading.

Sample	Young's Modulus (MPa)	Tensile Strength (MPa)	Elongation at Break (%)	Flexural Modulus (MPa)
R3	6.56 ± 0.14	1.50 ± 0.17	23.4 ± 2.4	6.54 ± 0.11
R3-D5	6.23 ± 0.14	1.40 ± 0.12	22.8 ± 1.6	6.97 ± 0.13
R3-D10	6.33 ± 0.25	1.33 ± 0.10	22.1 ± 1.5	6.47 ± 0.39
R3-D23	5.83 ± 0.13	0.87 ± 0.11	15.5 ± 1.8	6.74 ± 0.18
R1-D30	5.87 ± 0.17	0.83 ± 0.22	14.4 ± 3.5	6.97 ± 0.18

Table S4 – Mechanical properties of nanocomposites printed with resin R3 as the matrix. Data are expressed as mean ± SD, obtained by averaging five replicate measurements for each composition.

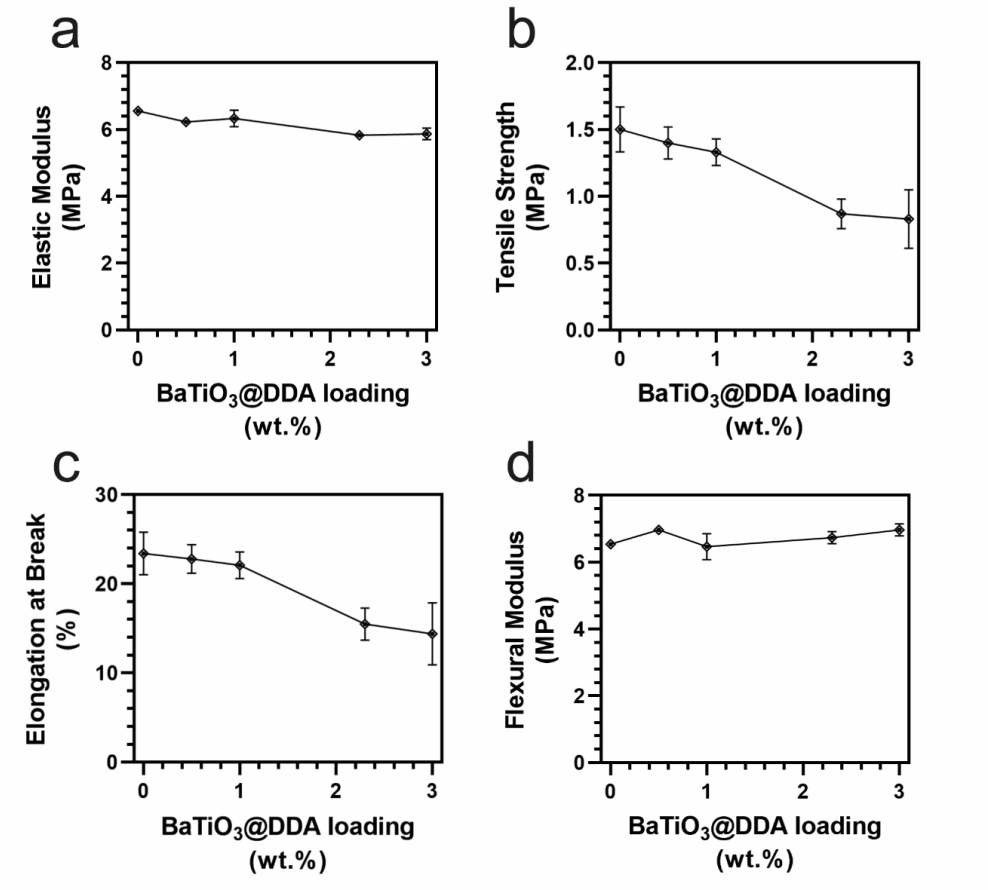

Figure S14. a) Young's modulus; b) tensile strength, c) elongation at break and d) flexural modulus of BTO-DDA nanocomposites prepared using R3 as polymer matrix as a function of BTO-DDA loading.

	NO POLING Layer thickness 0.05 mm			
	d_{33} (pC/N)			
f (Hz)	**R1**	**R1-D5**	**R1-D10**	**R1-D30**
200	0.2	1.3	0.3	1.4
271	0.2	1.5	0.4	1.2
343	0.2	1.05	0.1	1.25
414	0.2	1.1	0.3	1.15
486	0.015	0.95	0.4	1.15
557	0.1	0.7	0.7	0.85
629	0.025	1.65	0.6	1.75
700	0.2	1.3	0.7	1.2
771	0.1	1.2	0.95	1.0
843		1.05	1.2	0.95
914		0.95	1.4	0.75
986		0.85	1.7	0.3
1057		0.8	2.45	
1129		0.7	2.5	
1200		0.5	2.75	

Table S5 – Piezoelectric characterization of non-poled samples. The table reports d_{33} values (pC/N) as a function of the testing frequency f (Hz). Data plotted in Figure 8a.

	POLING at 1.0 kV Layer thickness 0.05 mm				
	d_{33} (pC/N)				
f (Hz)	**R1**	**R1-D5**	**R1-D10**	**R1-D30**	**R1-D50**
200	1.1	15.1	15.0	31.4	13.0
271	1.0	16.6	14.8	24.9	9.5
343	1.5	15.1	15.0	29.3	7.0
414	1.1	14.3	14.5	26.4	1.5
486	1.0	13.1	13.4	22.7	1.6
557	1.0	10.7	14.0	19.4	1.4
629	1.5	21.8	26.0	**42.3**	8.7
700	1.5	18.2	18.4	32.8	3.6
771	1.5	16.6	17.5	30.6	3.7
843	1.5	16.5	17.1	29.4	3.7
914	1.4	15.4	16.6	27.3	3.8
986	1.4	14.1	14.9	24.9	4.9
1057	1.6	18.3	21.2	32.6	2.6
1129	1.5	14.6	15.8	23.4	3.3
1200	1.5	13.9	15.3	22.3	3.0

Table S6 – Piezoelectric characterization of samples poled at 1 kV. The table reports d_{33} values (pC/N) as a function of the testing frequency f (Hz). Data plotted in Figure 8b.

	POLING at 1.2 kV						
	d_{33} (pC/N)						
f (Hz)	**R1** 0.05 mm	**R1- D5** 0.05 mm	**R1-D10** 0.05 mm	**R1-D10** 0.025 mm	**R1-D30** 0.05 mm	**R1-D30** 0.025 mm	**R1-D50** 0.05 mm
200	0.3	24.4	27.5	0.5	48.8	9.9	3.0
271	0.2	21.8	26.8	1	58.0	12.0	2.3
343	0.5	16.6	19.6	0.45	35.0	9.3	2.9
414	0.45	15.0	20.4	0.5	36.9	9.7	2.6
486	0.3	14.5	19.2	0.55	34.0	8.8	2.1
557	0.2	9.3	14.0	0.5	26.9	8.0	1.5
629	0.65	19.6	25.5	1	**51.7**	16.9	3.1
700	0.45	17.9	27.6	0.55	50.0	13.5	3.0
771	0.4	17.0	24.0	0.55	43.4	12.0	2.4
843	0.5	16.2	24.1	0.4	43.9	11.0	2.3
914	0.55	13.6	21.0	0.45	39.3	10.6	1.8
986	0.4	12.5	18.5	0.5	36.5	9.8	1.0
1057	0.1	11.0	16.5	0.45	34.4	9.8	0.8
1129	0.25	10.1	17.7	0.55	37.8	10.0	0.8
1200	0.2	9.7	13.9	0.5	29.5	9.6	1.1

Table S7 – Piezoelectric characterization of samples poled at 1.2 kV with different layer thickness. The table reports d_{33} values (pC/N) as a function of the testing frequency f (Hz). Data plotted in Figure 8c-d.

	Average d_{33} (pC/N)			
BTO – DDA loading	**Not poled Layer: 0.05 mm**	**Poling: 1 kV Layer: 0.05 mm**	**Poling: 1.2 kV Layer: 0.05 mm**	**Poling: 1.2 kV, Layer: 0.025 mm**
0%	0.1	1.3	0.4	
0.5%	1.0	15.6	15.3	
1%	1.1	16.6	21.1	0.6
3%	1.1	28.0	40.4	10.7
5%		4.8	2.0	

Table S8 – Piezoelectric coefficients, averaged through all the explored frequency range. Data plotted in Figure 8e.

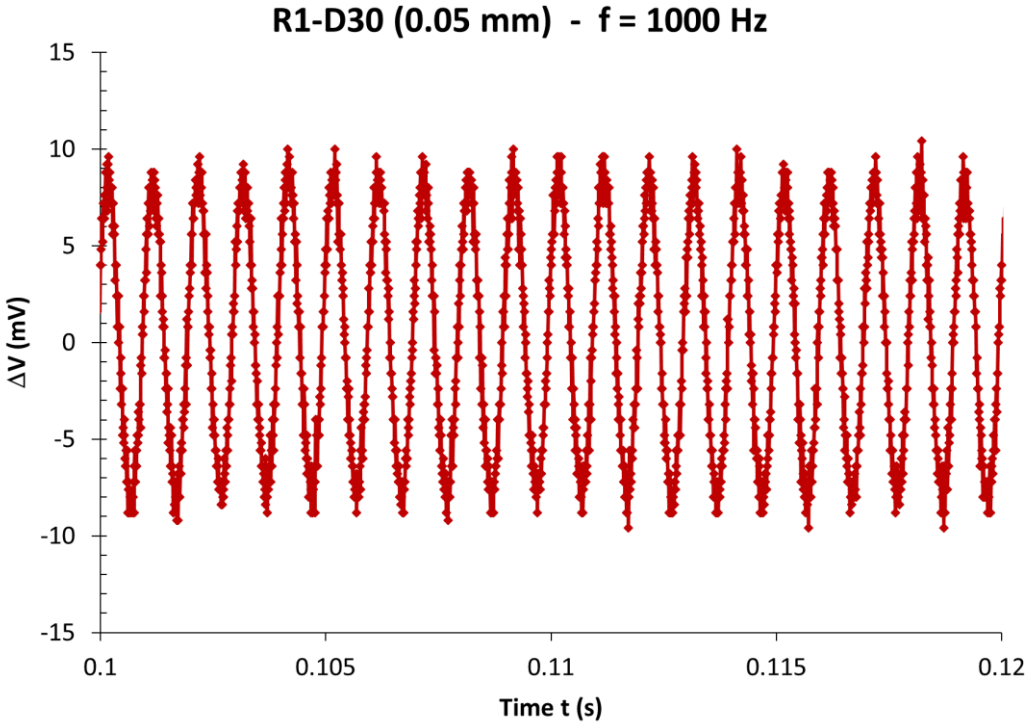

Figure S15 – Piezoelectric response of R1-D30 (0.05 mm) specimen, two years after its production, tested at 1 kHz (C_f = 0.15 nF), resulting in a d_{33} = 33.7 pC/N.